Molecular Cell, *Volume 39*

Supplemental Information

MAGE-RING Protein Complexes Comprise a Family of E3 Ubiquitin Ligases

Jennifer M. Doyle, Jinlan Gao, Jiawei Wang, Maojun Yang, and Patrick Ryan Potts

A

MAGE	A1	A2	A3	A4	A6	A8	A9	A10	A11	A12	B1	B2	B3	B4	B5	B6	B10	B16	B18	C1	C2	C3	D1	D2	D3	D4	E1	E2	F1	G1	H1	L2	NDN	MMS21
A1	100	76	75	80	76	77	71	68	67	77	54	51	55	58	47	49	55	56	53	53	53	55	42	41	42	42	39	30	37	42	21	37	30	2
A2	76	100	84	71	84	70	65	62	61	91	46	48	45	51	43	42	52	49	48	48	50	51	39	38	38	38	37	28	37	41	22	37	28	4
A3	75	84	100	69	94	67	64	58	60	84	46	47	45	50	42	43	49	47	47	50	50	51	40	41	40	40	39	29	37	41	25	38	29	3
A4	80	71	69	100	69	77	72	63	66	71	54	52	53	54	46	48	56	56	51	53	52	49	42	40	42	43	40	29	39	43	23	37	30	2
A6	76	84	94	69	100	67	63	59	60	84	46	47	45	50	41	42	49	47	47	51	50	51	39	40	40	38	40	30	38	41	25	38	30	4
A8	77	70	67	77	67	100	75	70	66	71	50	50	52	54	44	47	55	54	53	52	51	57	45	41	43	46	40	31	37	44	22	38	31	2
A9	71	65	64	72	63	75	100	66	67	64	50	48	53	55	47	46	56	55	52	54	56	56	41	37	41	43	37	29	38	40	20	37	30	2
A10	68	62	58	63	59	70	66	100	67	61	53	48	54	60	47	46	58	56	53	56	56	57	40	41	40	40	38	31	37	43	22	36	33	2
A11	67	61	60	66	60	66	67	67	100	60	50	47	54	55	46	47	55	57	54	56	54	51	45	44	45	42	41	33	41	45	24	38	31	4
A12	77	91	84	71	84	71	64	61	60	100	49	48	47	52	43	44	53	50	47	49	48	49	40	39	40	40	35	30	36	40	23	37	29	4
B1	54	46	46	54	46	50	50	53	50	49	100	64	59	70	55	59	60	57	58	45	49	41	40	44	44	43	38	33	39	44	23	38	36	8
B2	51	48	47	52	47	50	48	48	47	48	64	100	57	65	50	51	55	55	55	46	51	44	39	43	44	42	41	36	45	42	25	38	31	2
B3	55	45	45	53	45	52	53	54	54	47	59	57	100	64	61	56	58	61	57	47	48	41	46	44	47	48	38	35	42	45	25	40	34	3
B4	58	51	50	54	50	54	55	60	55	52	70	65	64	100	60	57	61	60	58	47	51	48	43	48	48	46	43	33	43	47	25	44	37	3
B5	47	43	42	46	41	44	47	47	46	43	55	50	61	60	100	52	53	53	51	41	41	34	39	40	44	41	39	28	38	42	23	38	33	5
B6	49	42	43	48	42	47	46	46	47	44	59	51	56	57	52	100	51	52	53	41	43	40	43	45	47	46	40	34	41	42	26	40	37	2
B10	55	52	49	56	49	55	56	58	55	53	60	55	58	61	53	51	100	64	63	54	51	45	43	45	47	45	42	35	41	46	25	39	36	5
B16	56	49	47	56	47	54	55	56	57	50	57	55	61	60	53	52	64	100	63	50	51	44	44	47	47	46	44	36	43	49	25	40	37	3
B18	53	48	47	51	47	53	52	53	54	47	58	55	57	58	51	53	63	63	100	48	53	44	44	43	44	45	40	34	43	42	25	38	34	3
C1	53	48	50	53	51	52	54	56	56	49	45	46	47	47	41	41	54	50	48	100	69	66	40	42	43	39	38	31	38	40	25	34	33	2
C2	53	50	50	52	50	51	56	56	54	48	49	51	48	51	41	43	51	51	53	69	100	64	40	40	39	39	39	30	38	41	26	37	32	3
C3	55	51	51	49	51	57	56	57	51	49	41	44	41	48	34	40	45	44	44	66	64	100	37	42	39	35	36	25	36	38	12	37	25	3
D1	42	39	40	42	39	45	41	40	45	40	40	39	46	43	39	43	43	44	44	40	40	37	100	78	76	78	46	38	47	43	25	49	37	4
D2	41	38	41	40	40	41	37	41	44	39	44	43	44	48	40	45	45	47	43	42	40	42	78	100	79	67	48	34	49	48	30	51	43	4
D3	42	38	40	42	40	43	41	40	45	40	44	44	47	48	44	47	47	47	44	43	39	39	76	79	100	74	47	34	48	47	30	48	43	5
D4	42	38	40	43	38	46	43	40	42	40	43	42	48	46	41	46	45	46	45	39	39	35	78	67	74	100	40	38	45	46	25	44	39	3
E1	39	37	39	40	40	40	37	38	41	35	38	41	38	43	39	40	42	44	40	38	39	36	46	48	47	40	100	38	54	47	29	44	34	2
E2	30	28	29	29	30	31	29	31	33	30	33	36	35	33	28	34	35	36	34	31	30	25	38	34	34	38	38	100	34	39	25	36	28	7
F1	37	37	37	39	38	37	38	37	41	36	39	45	42	43	38	41	41	43	43	38	38	36	47	49	48	45	54	34	100	59	27	50	45	2
G1	42	41	41	43	41	44	40	43	45	40	44	42	45	47	42	42	46	49	42	40	41	38	43	48	47	46	47	39	59	100	27	50	42	2
H1	21	22	25	23	25	22	20	22	24	23	23	25	25	25	23	26	25	25	25	25	26	12	25	30	30	25	29	25	27	27	100	25	26	5
L2	37	37	38	37	38	38	37	36	38	37	38	38	40	44	38	40	39	40	38	34	37	37	49	51	48	44	44	36	50	50	25	100	39	2
NDN	30	28	29	30	30	31	30	33	31	29	36	31	34	37	33	37	36	37	34	33	32	25	37	43	43	39	34	28	45	42	26	39	100	1
MMS21	2	4	3	2	4	2	2	2	4	4	8	2	3	3	5	2	5	3	3	2	3	3	4	4	5	3	2	7	2	2	5	2	1	100

B

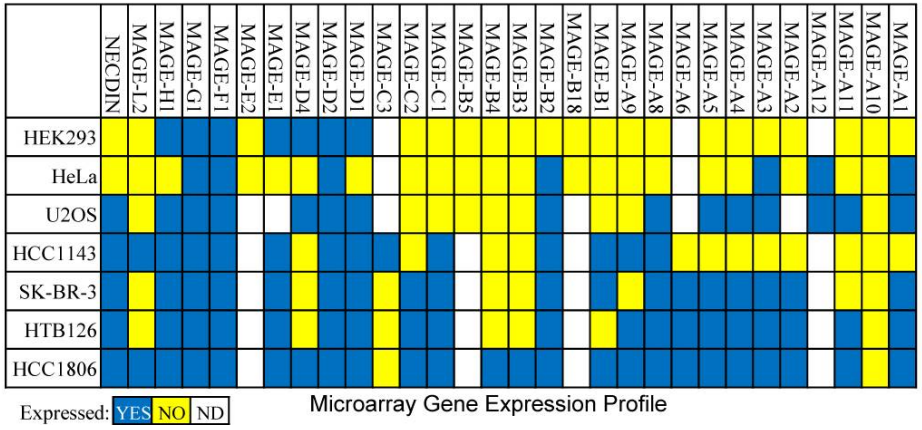

Figure S1. Similarity and expression profile of various MAGEs. (Related to Figure 1)

(A) The MHDs of the indicated MAGEs were aligned by clustalW and the percentage of identical amino acids between the various MHDs is given and colored on a three color scale (blue = high, yellow = medium, red = low). MMS21 (amino acids 1-170) was included as an irrelevant protein to show high conservation between various MHDs.

(B) Microarray gene expression profiles of the indicated cell lines were analyzed for the expression of the indicated MAGEs. Blue = expressed, yellow = not expressed, and white = not determined (N.D). Expression of MAGEs in HEK293, HeLa, and U2OS cells was based off of multiple previously published microarrays for each cell line (Carson et al., 2004; El Hader et al., 2005; Elkon et al., 2005; Kim et al., 2007a; Kim et al., 2007b; Monroe et al., 2005). Expression of MAGEs in HCC1143, HCC1806, HTB126, and SK-BR-3 cells was determined by Affymetrix microarrays

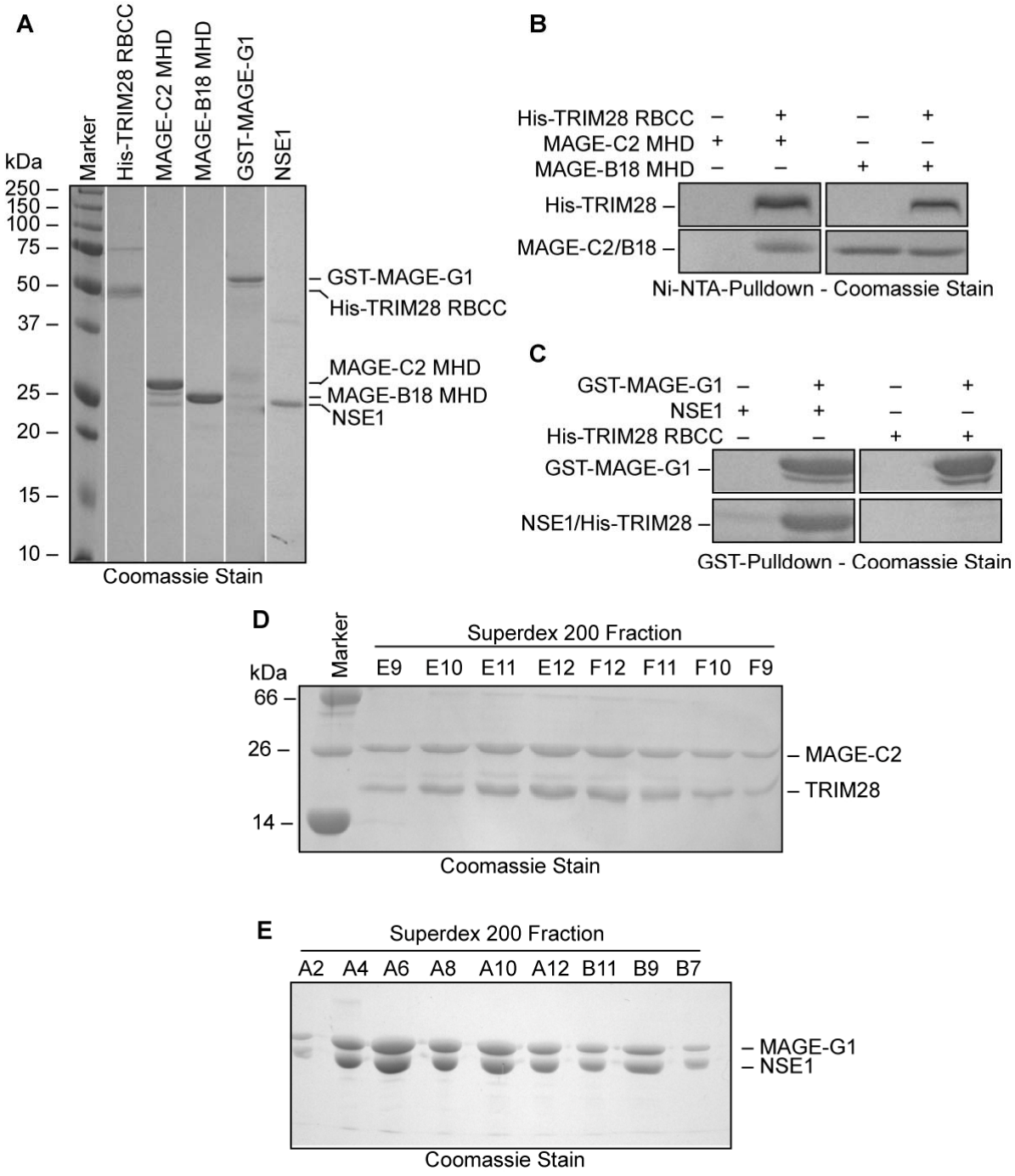
A
Marker
His-TRIM28 RBCC
MAGE-C2 MHD
MAGE-B18 MHD
GST-MAGE-G1
NSE1
kDa
250 –
150 –
100 –
75 –
50 –
37 –
25 –
20 –
15 –
10 –
– GST-MAGE-G1
His-TRIM28 RBCC
MAGE-C2 MHD
MAGE-B18 MHD
NSE1
Coomassie Stain
B
His-TRIM28 RBCC – + – +
MAGE-C2 MHD + + – –
MAGE-B18 MHD – – + +
His-TRIM28 –
MAGE-C2/B18 –
Ni-NTA-Pulldown - Coomassie Stain
C
GST-MAGE-G1 – + – +
NSE1 + + – –
His-TRIM28 RBCC – – + +
GST-MAGE-G1 –
NSE1/His-TRIM28 –
GST-Pulldown - Coomassie Stain
D
Marker
Superdex 200 Fraction
kDa
E9 E10 E11 E12 F12 F11 F10 F9
66 –
26 –
14 –
– MAGE-C2
– TRIM28
Coomassie Stain
E
Superdex 200 Fraction
A2 A4 A6 A8 A10 A12 B11 B9 B7
– MAGE-G1
– NSE1
Coomassie Stain

Figure S2. MAGE and RING proteins directly bind one another *in vitro*. (Related to Figure 2).

(A) Recombinant MAGE and RING proteins purified from *E. coli*. His-TRIM28 RBCC (AA 33-413) was purified over Ni-NTA agarose, eluted with 250 mM imidazole, and further purified by size exclusion chromatography. GST-MAGE-G1 was purified over glutathione sepharose, eluted with 10 mM glutathione, and further purified by size exclusion chromatography. MAGE-B18 MHD (AA 101-331) and MAGE-C2 MHD (AA 140-373) were expressed as His-tagged proteins, purified over Ni-NTA agarose, cleaved off the beads with TEV protease, and subjected to size exclusion chromatography. NSE1 was expressed as a GST-tagged protein, purified over glutathione sepharose, and cleaved off the beads with prescission protease. All proteins were separated by SDS-PAGE and coomassie stained.

(B) MAGE-C2 directly binds His-TRIM28 RBCC. The indicated recombinant proteins (shown in (A)) were incubated for one hour at room temperature and then captured with Ni-NTA agarose. Bound proteins were washed with 20 mM imidazole, eluted with SDS sample buffer, separated by SDS-PAGE, and detected by coomassie staining. Note, a fraction of MAGE-B18 showed non-specific binding to Ni-NTA, but no enhancement upon addition of His-TRIM28 RBCC.

(C) MAGE-G1 directly binds GST-MAGE-G1. The indicated recombinant proteins (shown in (A)) were incubated for one hour at room temperature and captured with glutathione sepharose. Bound proteins were washed, eluted with SDS sample buffer, separated by SDS-PAGE, and detected by coomassie staining.

(D) Recombinant MAGE-C2 and TRIM28 form a complex. MAGE-C2 (AA 140-373) and His-TRIM28 (AA 247-382) were co-expressed in *E. coli*. Cell lysates were incubated with Ni-NTA agarose and the MAGE-C2-TRIM28 complex was cleaved off the beads with TEV protease and

further purified by size exclusion chromatography (Superdex 200). The indicated fractions were separated by SDS-PAGE and stained with coomassie blue.

(E) Recombinant MAGE-G1 and NSE1 form a complex. Full-length His-MAGE-G1 and NSE1 were co-expressed and purified as described in (D).

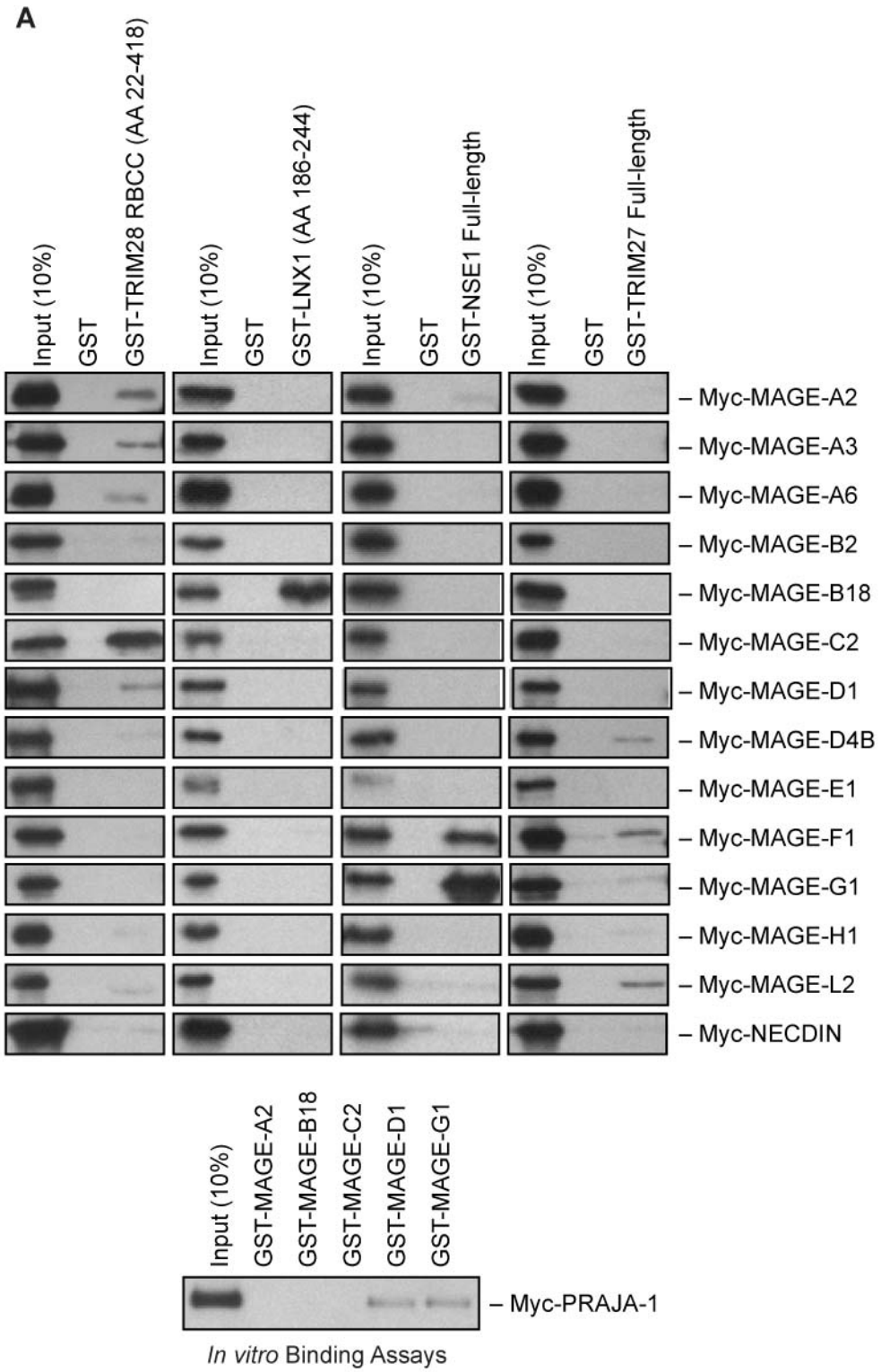
A
Input (10%)
GST
GST-TRIM28 RBCC (AA 22-418)
Input (10%)
GST
GST-LNX1 (AA 186-244)
Input (10%)
GST
GST-NSE1 Full-length
Input (10%)
GST
GST-TRIM27 Full-length
– Myc-MAGE-A2
– Myc-MAGE-A3
– Myc-MAGE-A6
– Myc-MAGE-B2
– Myc-MAGE-B18
– Myc-MAGE-C2
– Myc-MAGE-D1
– Myc-MAGE-D4B
– Myc-MAGE-E1
– Myc-MAGE-F1
– Myc-MAGE-G1
– Myc-MAGE-H1
– Myc-MAGE-L2
– Myc-NECDIN
Input (10%)
GST-MAGE-A2
GST-MAGE-B18
GST-MAGE-C2
GST-MAGE-D1
GST-MAGE-G1
– Myc-PRAJA-1
In vitro Binding Assays

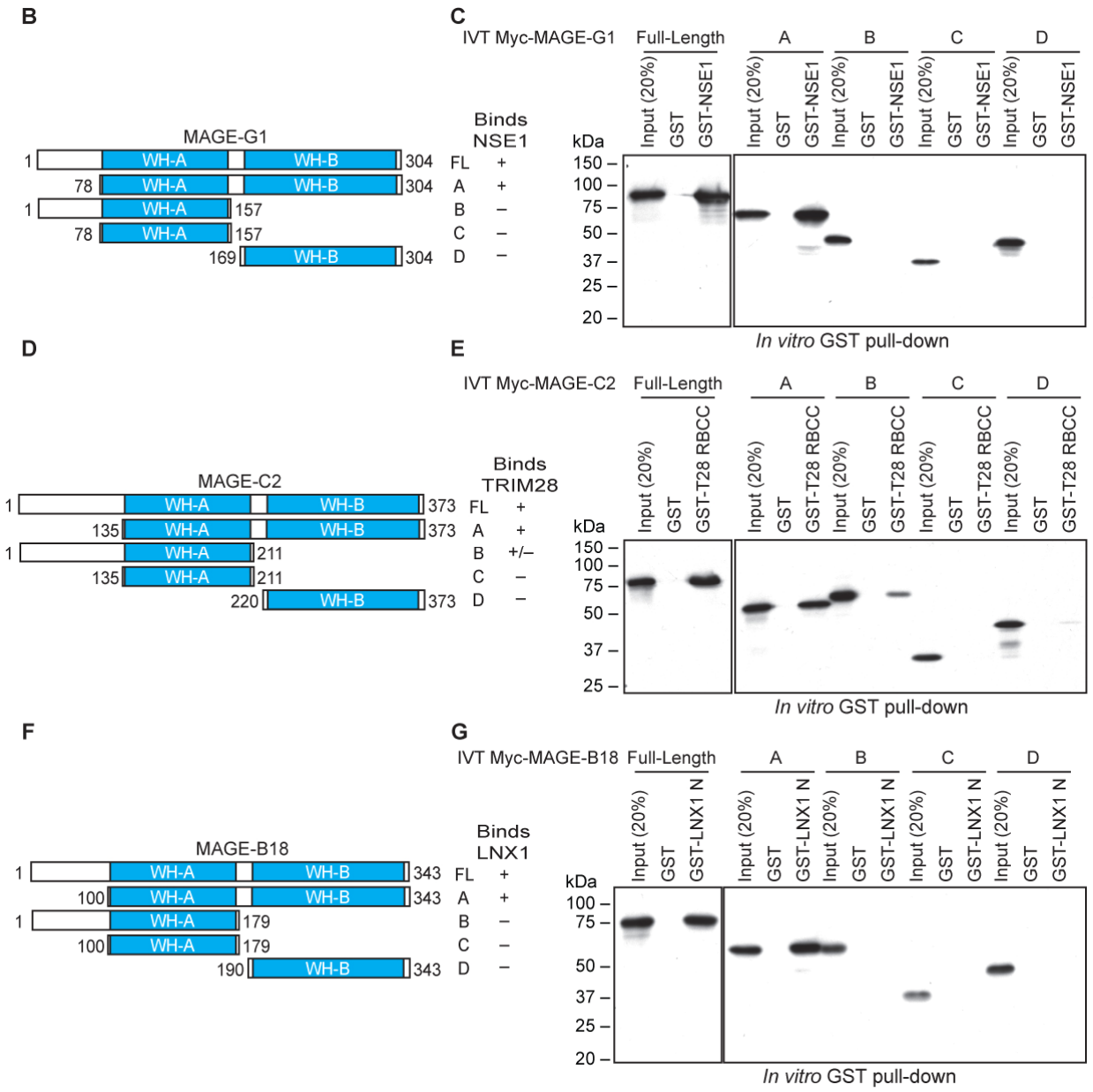
B
MAGE-G1
1
WH-A
WH-B
304
78
304
1
157
78
157
169
304
Binds NSE1
FL +
A +
B –
C –
D –
C
IVT Myc-MAGE-G1
Full-Length
A
B
C
D
Input (20%)
GST
GST-NSE1
kDa
150 –
100 –
75 –
50 –
37 –
25 –
20 –
In vitro GST pull-down
D
MAGE-C2
1
WH-A
WH-B
373
135
373
1
211
135
211
220
373
Binds TRIM28
FL +
A +
B +/–
C –
D –
E
IVT Myc-MAGE-C2
Full-Length
A
B
C
D
Input (20%)
GST
GST-T28 RBCC
kDa
150 –
100 –
75 –
50 –
37 –
25 –
In vitro GST pull-down
F
MAGE-B18
1
WH-A
WH-B
343
100
343
1
179
100
179
190
343
Binds LNX1
FL +
A +
B –
C –
D –
G
IVT Myc-MAGE-B18
Full-Length
A
B
C
D
Input (20%)
GST
GST-LNX1 N
kDa
100 –
75 –
50 –
37 –
25 –
20 –
In vitro GST pull-down

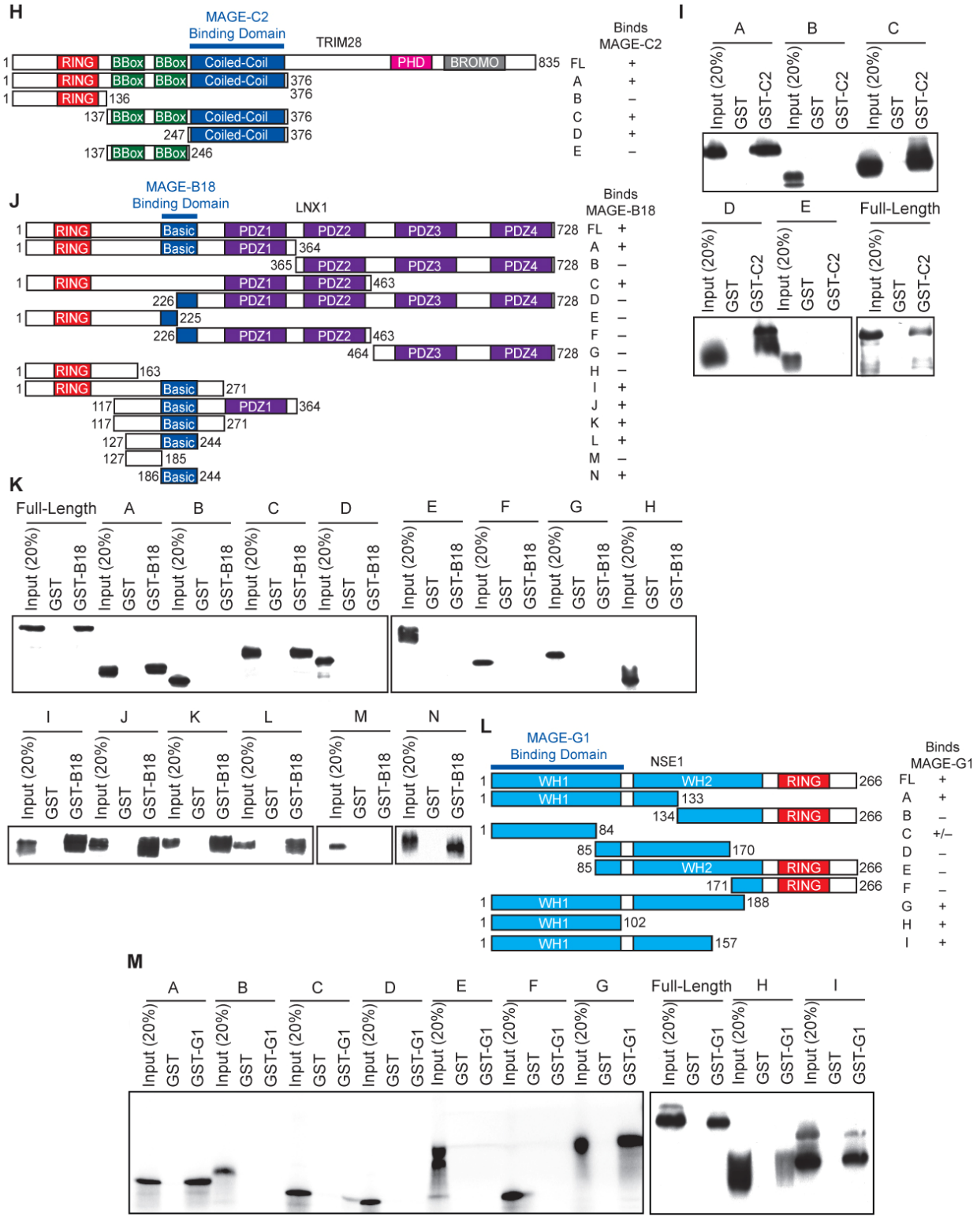
H
MAGE-C2 Binding Domain
TRIM28
Binds MAGE-C2
RING
BBox
Coiled-Coil
PHD
BROMO
FL +
A +
B –
C +
D +
E –
I
A
B
C
Input (20%)
GST
GST-C2
D
E
Full-Length
J
MAGE-B18 Binding Domain
LNX1
Binds MAGE-B18
Basic
PDZ1
PDZ2
PDZ3
PDZ4
FL +
A +
B –
C +
D –
E –
F –
G –
H –
I +
J +
K +
L +
M –
N +
K
Full-Length
GST-B18
L
MAGE-G1 Binding Domain
NSE1
Binds MAGE-G1
WH1
WH2
RING
FL +
A +
B –
C +/–
D –
E –
F –
G +
H +
I +
M
GST-G1

Figure S3. MAGE-RING specificity and interaction mapping. (Related to Figure 3)

(A) GST, GST-E3 RING domain proteins (GST-TRIM28 RBCC (AA 22-418), GST-LNX1 (AA186-244), GST-NSE1 full-length, GST-TRIM27 full-length) (Top), or full-length GST-MAGE proteins (bottom) were bound to glutathione sepharose beads and incubated with the indicated *in vitro* translated proteins. Interacting Myc-proteins were detected by SDS-PAGE followed by immunoblotting with an anti-Myc antibody.

(B) Mapping regions on MAGE-G1 necessary for binding NSE1 RING protein. Schematic of various MAGE-G1 fragments used in *in vitro* binding assays.

(C) GST or GST-NSE1 were bound to glutathione sepharose and incubated with the indicated *in vitro* translated (IVT) fragments of Myc-MAGE-G1. Interacting fragments of Myc-MAGE-G1 were detected by SDS-PAGE followed by immunoblotting with an anti-Myc antibody. Input denotes 20% of total IVT protein.

(D) Mapping regions on MAGE-C2 necessary for binding TRIM28 RING protein. Schematic of various MAGE-C2 fragments used in *in vitro* binding assays.

(E) *In vitro* binding assays were performed as described in (C) except with GST or GST-TRIM28 RBCC (amino acids 22-418) and IVT fragments of Myc-MAGE-C2.

(F) Mapping regions on MAGE-B18 necessary for binding LNX1 RING protein Schematic of various MAGE-B18 fragments used in *in vitro* binding assays.

(G) *In vitro* binding assays were performed as described in (C) except with GST or GST-LNX1 fragment N (amino acids 186-244) and IVT fragments of Myc-MAGE-B18

(H) Schematic of various TRIM28 fragments used in *in vitro* binding assays.

(I) GST or GST-MAGE-C2 were bound to glutathione sepharose and incubated with the indicated *in vitro* translated (IVT) fragments of Myc-TRIM28. Interacting fragments of Myc-TRIM28 were detected by SDS-PAGE followed by immunoblotting with an anti-Myc antibody.

Equal loading of GST and GST-MAGE-C2 was confirmed by immunoblotting with an anti-GST antibody (data not shown). Input denotes 20% of total IVT protein.

(J) Schematic of various LNX1 fragments used in *in vitro* binding assays.

(K) *In vitro* binding assays were performed as described in (I) except with GST or GST-MAGE-B18 and IVT fragments of Myc-LNX1.

(L) Schematic of various NSE1 fragments used in *in vitro* binding assays.

(M) *In vitro* binding assays were performed as described in (I) except with GST or GST-MAGE-G1 and IVT fragments of Myc-NSE1.

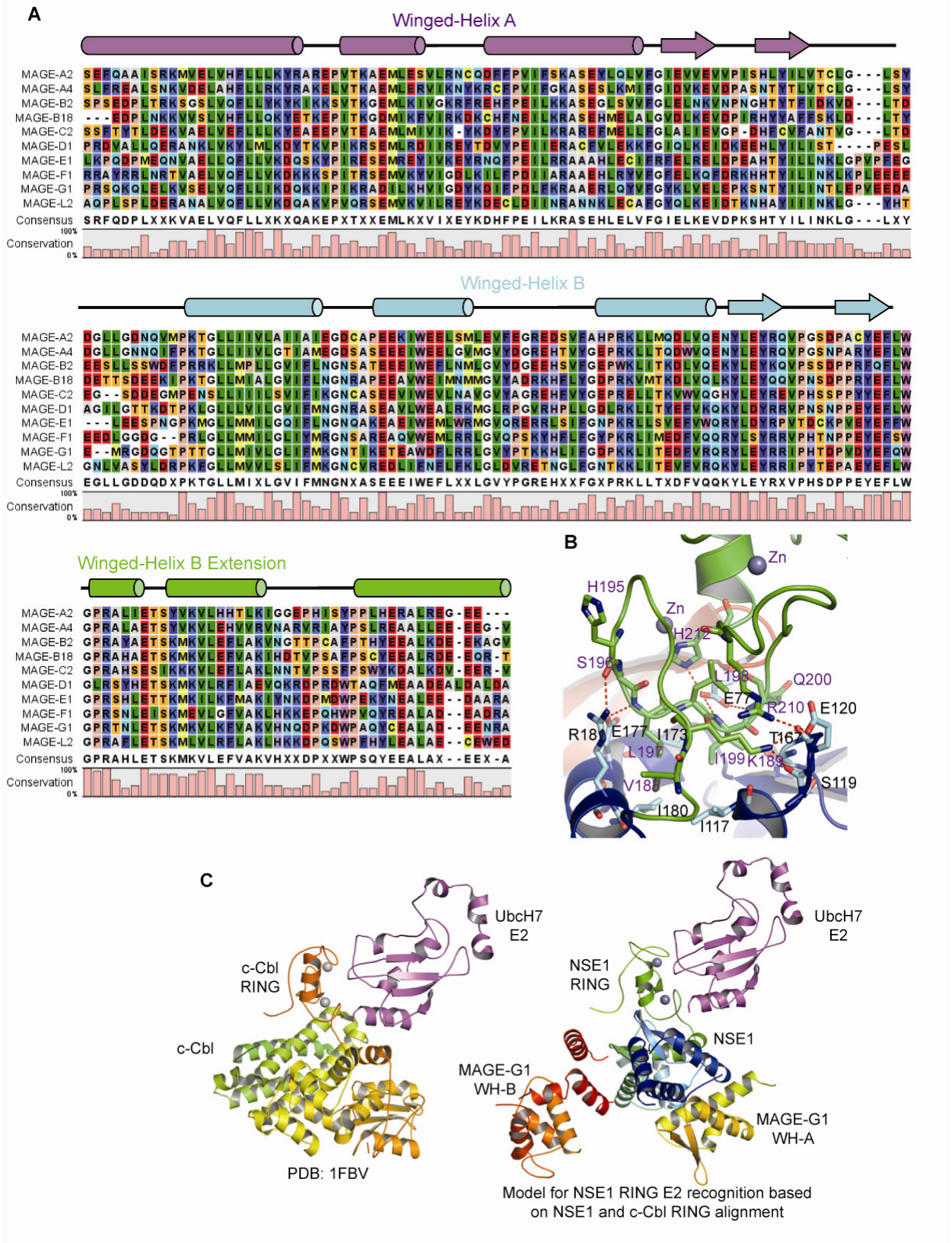
A
Winged-Helix A
MAGE-A2
MAGE-A4
MAGE-B2
MAGE-B18
MAGE-C2
MAGE-D1
MAGE-E1
MAGE-F1
MAGE-G1
MAGE-L2
Consensus
Conservation
Winged-Helix B
Winged-Helix B Extension
B
Zn
H195
H212
S196
L198
Q200
E77
R210
E120
R181
E177
I173
T167
L197
I199
K189
V188
S119
I180
I117
C
UbcH7
E2
c-Cbl
RING
c-Cbl
PDB: 1FBV
NSE1
RING
NSE1
MAGE-G1
WH-B
MAGE-G1
WH-A
Model for NSE1 RING E2 recognition based
on NSE1 and c-Cbl RING alignment

Figure S4. MAGE homology domains contain WH-A and extended WH-B motifs.

(Related to Figure 4)

(A) Sequence alignment of various MAGE homology domains. The secondary structure derived from the crystal structure of MAGE-G1 is depicted above the sequence. Cylinders represent alpha-helices and arrows represent beta-sheets. The WH-A motif is shown in purple, the WH-B motif in cyan, and the WH-B extension in green.

(B) The NSE1 RING domain interacts with both NSE1 WH1 and WH2 motifs through a series of hydrogen bonds and with WH2 through a hydrophobic core. E77 of WH1 forms three ionic bonds with the side chain of H212 and the main chain of L198, I199, and Q200 in the RING domain. V188, L197 and I199 of the RING domain form a hydrophobic core that interact with the hydrophobic surface of I117, T167, I173, and I180 in the WH2 motif.

(C) NSE1 RING domain in MAGE-G1-NSE1 crystal structure is predicted to be accessible to E2 ubiquitin-conjugating enzymes. Left; Crystal structure (PDB: 1FBV)of c-Cbl bound to the UbcH7 E2 ubiquitin-conjugating enzyme. Right; The NSE1 and c-Cbl RING domains were aligned and the UbcH7 structure was superimposed onto the MAGE-G1-NSE1 structure.

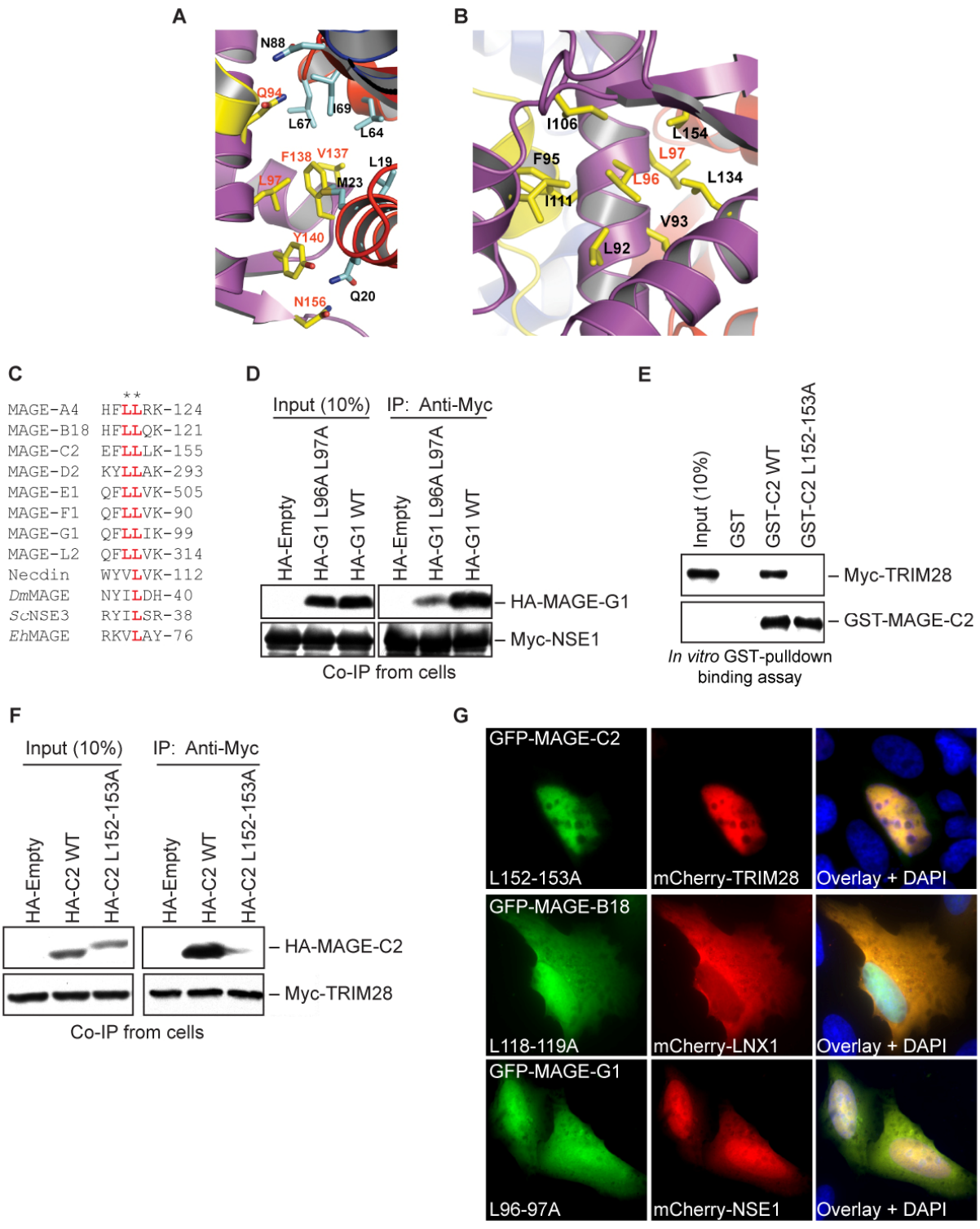
A
N88
Q94
I69
L67
L64
F138
V137
L19
L97
M23
Y140
N156
Q20
B
I106
L154
L97
F95
L96
L134
I111
V93
L92
C
MAGE-A4 HFLLRK-124
MAGE-B18 HFLLQK-121
MAGE-C2 EFLLLK-155
MAGE-D2 KYLLAK-293
MAGE-E1 QFLLVK-505
MAGE-F1 QFLLVK-90
MAGE-G1 QFLLIK-99
MAGE-L2 QFLLVK-314
Necdin WYVLVK-112
DmMAGE NYILDH-40
ScNSE3 RYILSR-38
EhMAGE RKVLAY-76
D
Input (10%)
IP: Anti-Myc
HA-Empty
HA-G1 L96A L97A
HA-G1 WT
– HA-MAGE-G1
– Myc-NSE1
Co-IP from cells
E
Input (10%)
GST
GST-C2 WT
GST-C2 L152-153A
– Myc-TRIM28
– GST-MAGE-C2
In vitro GST-pulldown binding assay
F
Input (10%)
IP: Anti-Myc
HA-Empty
HA-C2 WT
HA-C2 L152-153A
– HA-MAGE-C2
– Myc-TRIM28
Co-IP from cells
G
GFP-MAGE-C2
L152-153A
mCherry-TRIM28
Overlay + DAPI
GFP-MAGE-B18
L118-119A
mCherry-LNX1
Overlay + DAPI
GFP-MAGE-G1
L96-97A
mCherry-NSE1
Overlay + DAPI

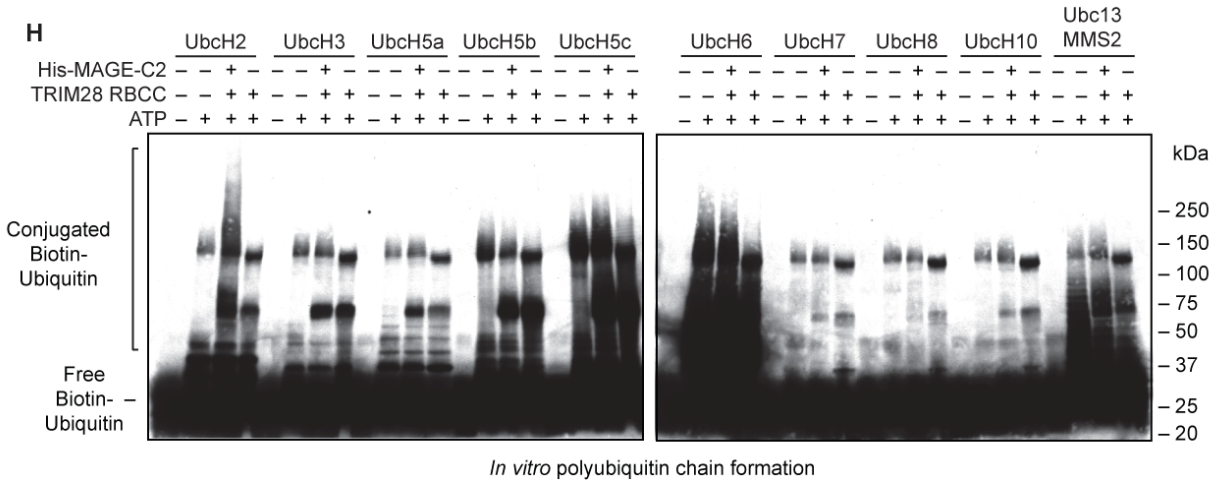

In vitro polyubiquitin chain formation

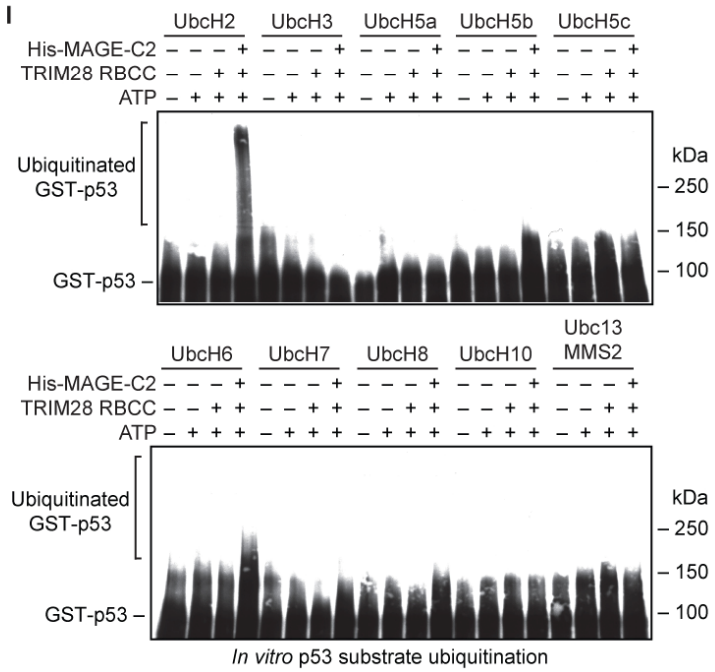

In vitro p53 substrate ubiquitination

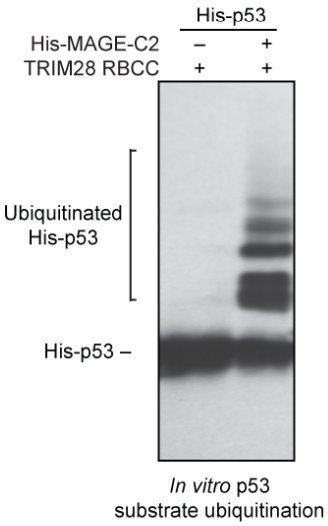

In vitro p53
substrate ubiquitination

Figure S5. MAGE di-leucine motif mutant characterization and determination of E2 ubiquitin-conjugating enzymes that function with MAGE-RING complexes *in vitro*. (Related to Figure 5)

(A) MAGE-G1-NSE1 binding interface. MAGE-G1 L97 is part of a hydrophobic core contacting NSE1.

(B) MAGE-G1 L96 is part of a hydrophobic core forming the WH-A motif.

(C) Conservation of the di-leucine motif (asterisks) in the indicated MAGE proteins. Amino acid numbers are shown.

(D) HeLa cells were transfected with the indicated HA-MAGE-G1 and Myc-NSE1 constructs for 36 hrs before Myc-NSE1 was immunoprecipitated with an anti-Myc antibody. HA-MAGE-G1 interaction was detected by immunoblotting with an anti-HA antibody.

(E) Mutation of MAGE-C2 L152 L153 disrupts interaction with TRIM28. The indicated GST-tagged MAGE-C2 proteins were bound to glutathione-sepharose and incubated with *in vitro* translated Myc-TRIM28. GST-MAGE-C2 and Myc-TRIM28 bound to the beads were detected by immunoblotting.

(F) Mutation of MAGE-C2 L152 L153 disrupts interaction with TRIM28 in cells. Immunoprecipitation of the indicated proteins was performed as described in (D).

(G) MAGE-C2, MAGE-B18, and MAGE-G1 di-leucine mutants still properly localize in cells. U2OS cells were transfected with the indicated GFP-MAGEs and mCherry-RING proteins. 48 hours after transfection cells were fixed and DNA stained with DAPI (blue). Images are representative of many fields.

(H) MAGE-C2 stimulates polyubiquitin chain formation by TRIM28 specifically in the presence of the UbcH2 E2 ubiquitin-conjugating enzyme. TRIM28 RBCC (AA 22-418) with or without

His-MAGE-C2 was incubated with biotinylated-ubiquitin, His_6-Ube1 (E1), Mg-ATP, and various E2 ubiquitin-conjugating enzymes for 1 hr at 37 °C. Polyubiquitin chains were detected by SDS-PAGE followed by probing with Streptavidin-conjugated horse radish peroxidase (HRP).

(I) MAGE-C2 stimulates GST-p53 ubiquitination by TRIM28 specifically in the presence of the UbcH2 E2 ubiquitin-conjugating enzyme. TRIM28 RBCC (AA 22-418) with or without His-MAGE-C2 was incubated with GST-p53, biotinylated-ubiquitin, His_6-Ube1 (E1), Mg-ATP, and various E2 ubiquitin-conjugating enzymes for 1 hr at 37 °C. GST-p53 was detected by anti-p53 immunoblotting.

(J) MAGE-C2-TRIM28 ubiquitinates His-p53. TRIM28 RBCC (AA 22-418) with or without MAGE-C2 was incubated with His-p53, biotinylated-ubiquitin, His_6-Ube1 (E1), Mg-ATP, and UbcH2 (E2) for 1 hr at 37 °C. His-p53 was detected by anti-p53 immunoblotting.

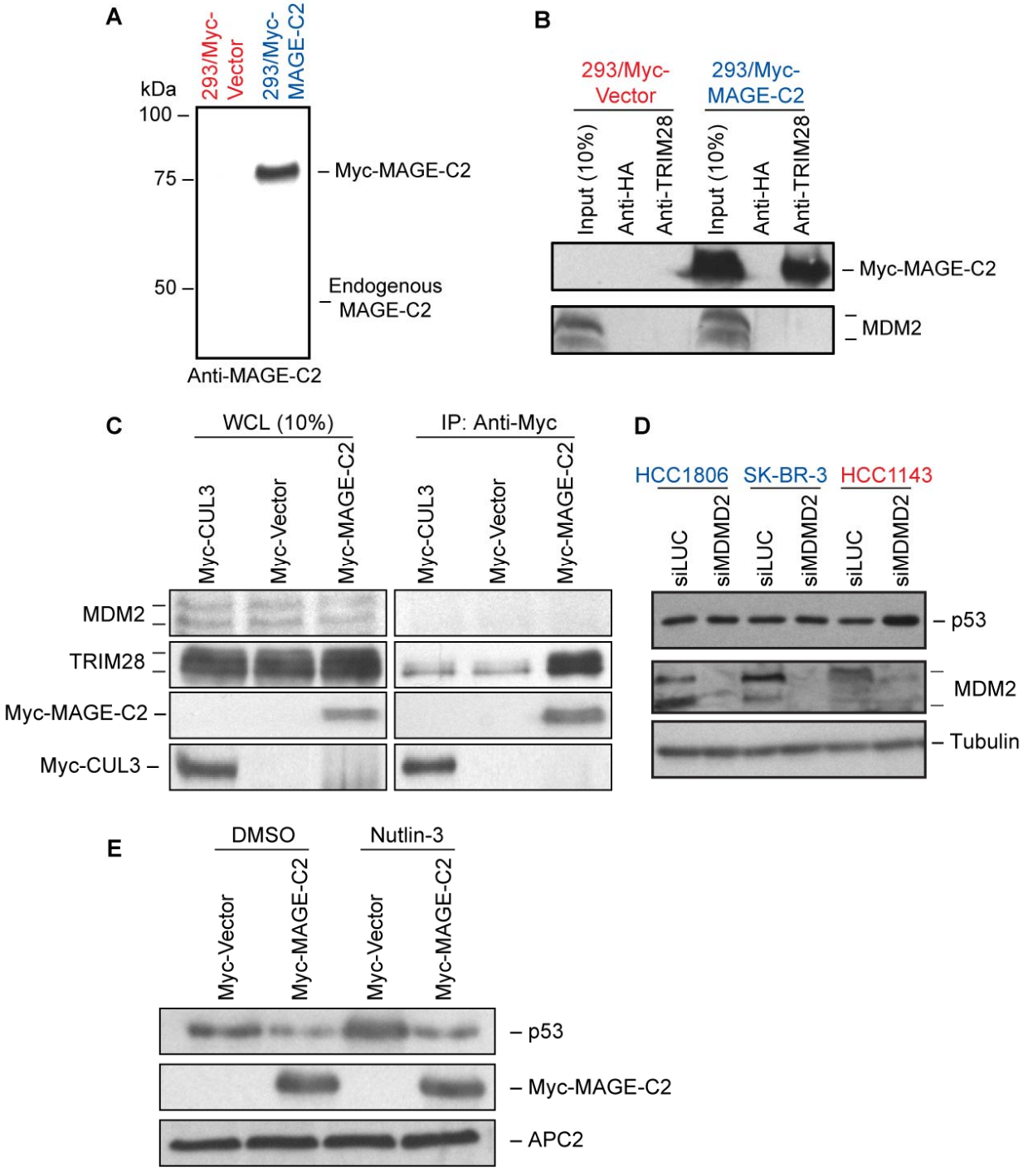
A
293/Myc-Vector
293/Myc-MAGE-C2
kDa
100 –
75 –
50 –
– Myc-MAGE-C2
Endogenous MAGE-C2
Anti-MAGE-C2
B
293/Myc-Vector
293/Myc-MAGE-C2
Input (10%)
Anti-HA
Anti-TRIM28
Input (10%)
Anti-HA
Anti-TRIM28
– Myc-MAGE-C2
MDM2
C
WCL (10%)
IP: Anti-Myc
Myc-CUL3
Myc-Vector
Myc-MAGE-C2
Myc-CUL3
Myc-Vector
Myc-MAGE-C2
MDM2
TRIM28
Myc-MAGE-C2 –
Myc-CUL3 –
D
HCC1806
SK-BR-3
HCC1143
siLUC
siMDMD2
siLUC
siMDMD2
siLUC
siMDMD2
– p53
MDM2
– Tubulin
E
DMSO
Nutlin-3
Myc-Vector
Myc-MAGE-C2
Myc-Vector
Myc-MAGE-C2
– p53
– Myc-MAGE-C2
– APC2

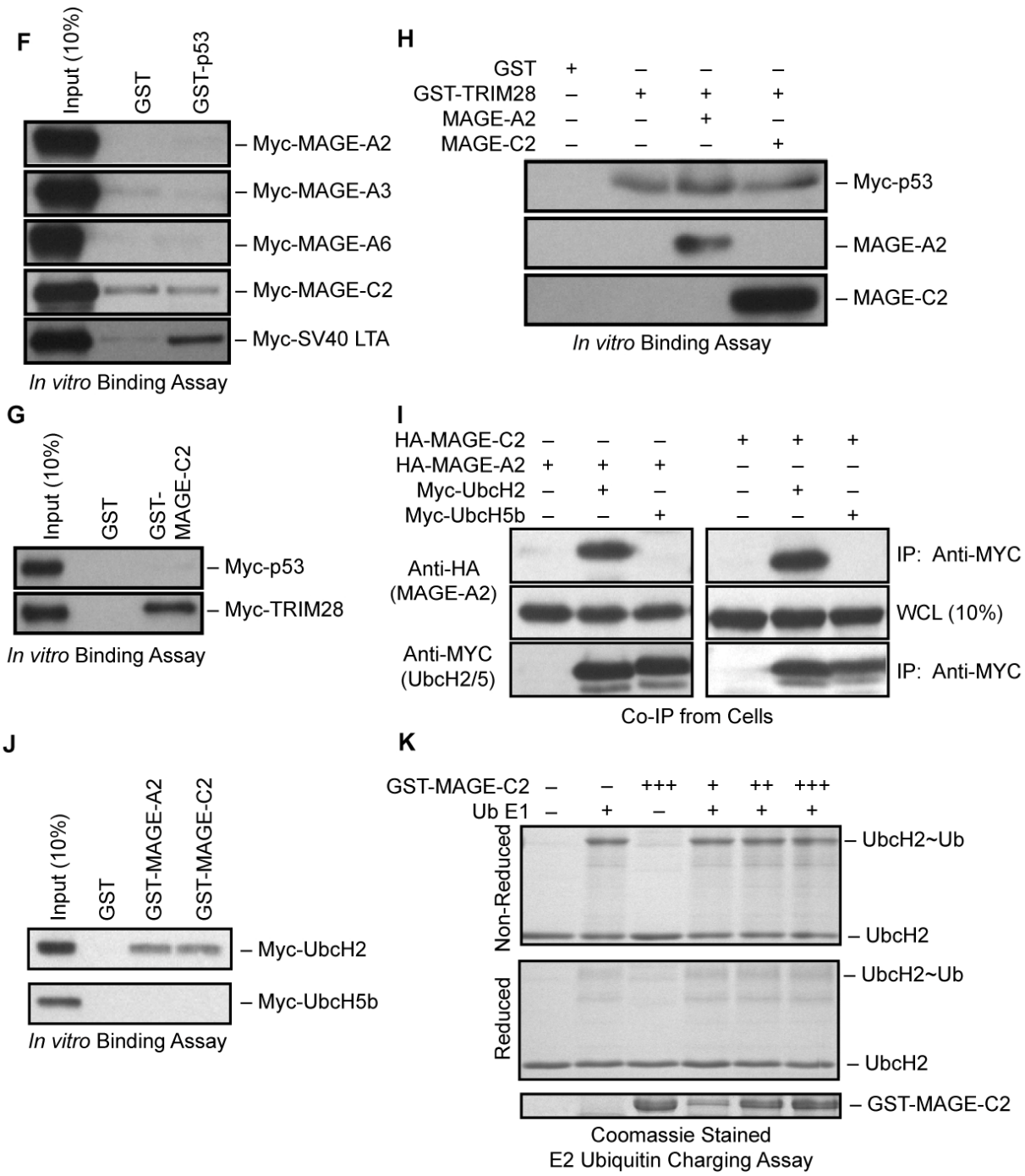
F
Input (10%)
GST
GST-p53
– Myc-MAGE-A2
– Myc-MAGE-A3
– Myc-MAGE-A6
– Myc-MAGE-C2
– Myc-SV40 LTA
In vitro Binding Assay
H
GST + – – –
GST-TRIM28 – + + +
MAGE-A2 – – + –
MAGE-C2 – – – +
– Myc-p53
– MAGE-A2
– MAGE-C2
In vitro Binding Assay
G
Input (10%)
GST
GST-MAGE-C2
– Myc-p53
– Myc-TRIM28
In vitro Binding Assay
I
HA-MAGE-C2 – – – + + +
HA-MAGE-A2 + + + – – –
Myc-UbcH2 – + – – + –
Myc-UbcH5b – – + – – +
Anti-HA (MAGE-A2)
Anti-MYC (UbcH2/5)
IP: Anti-MYC
WCL (10%)
IP: Anti-MYC
Co-IP from Cells
J
Input (10%)
GST
GST-MAGE-A2
GST-MAGE-C2
– Myc-UbcH2
– Myc-UbcH5b
In vitro Binding Assay
K
GST-MAGE-C2 – – +++ + ++ +++
Ub E1 – + – + + +
Non-Reduced
– UbcH2~Ub
– UbcH2
Reduced
– UbcH2~Ub
– UbcH2
– GST-MAGE-C2
Coomassie Stained
E2 Ubiquitin Charging Assay

Figure S6. Mechanistic insights into MAGE-C2 enhancement of TRIM28 E3 ubiquitin ligase activity. (Related to Figure 6)

(A) Characterization of HEK293/Myc-MAGE-C2 stable cell line. Cell lysates from 293/Myc-Vector or 293/Myc-MAGE-C2 stable cells was probed with an anti-MAGE-C2 antibody. Note HEK293 cells do not express endogenous MAGE-C2.

(B) MDM2 does not interact with TRIM28 or MAGE-C2-TRIM28. Cell lysates from 293/Myc-Vector or 293/Myc-MAGE-C2 stable cell lines were subjected to immunoprecipitation with anti-HA (negative control) or anti-TRIM28 antibodies followed by immunoblotting with anti-MAGE-C2 and anti-MDM2 antibodies. Note two bands detected by anti-MDM2 both disappear by RNAi (see panel (D)).

(C) MAGE-C2 does not associate with MDM2 in cells. HeLa cells were transfected with Myc-MAGE-C2 or the negative controls Myc-vector or Myc-CUL3. Forty-eight hours after transfection, cell lysates were subjected to immunoprecipitation with anti-Myc antibodies followed by immunoblotting with anti-Myc, anti-TRIM28 (positive control), and anti-MDM2. Note, Myc-MAGE-C2 associated with endogenous TRIM28, but not MDM2.

(D) Knockdown of MDM2 increases p53 protein levels in HCC1143 MAGE-negative cells (see Figures 6A and S1B), but not in HCC1806 and SK-BR-3 MAGE-positive cells (see Figures 6A and S1B). HCC1143, HCC1806, or SK-BR-3 cells were transfected with siLuciferase (siLUC) or siMDM2 RNAi oligonucleotides. p53, MDM2, and Tubulin (loading control) were detected by SDS-PAGE followed by immunoblotting 72 hours after transfection.

(E) MAGE-C2-induced p53 protein instability does not require MDM2. HCC1143 (MAGE-C2-negative cells) were transfected with Myc-vector or Myc-MAGE-C2 for 24 hours before addition of DMSO (control) or 10 μM Nutlin-3 (Sigma). Twenty-four hours after drug addition, cell

lysates were collected, subjected to SDS-PAGE, and immunoblotted for p53, Myc-MAGE-C2, and APC2 as a loading control. Note Myc-MAGE-C2 decreased p53 protein levels in both DMSO and Nutlin-3 treated samples. Nutlin-3 treatment was effective at inhibiting MDM2-p53 interaction as evidenced by increased p53 protein levels upon treatment of Myc-vector HCC1143 cells with Nutlin-3 (first and third lanes).

(F) GST or GST-p53 were bound to glutathione sepharose beads and incubated with *in vitro* translated Myc-MAGE-A2, -A3, -A6, -C2, and a known p53 interacting protein SV40 large T-antigen. Interacting Myc-tagged proteins were detected by SDS-PAGE followed by immunoblotting with an anti-Myc antibody.

(G) *In vitro* binding assays were performed as described in (F) except GST-MAGE-C2 was used as bait for binding to *in vitro* translated Myc-p53 or the positive control Myc-TRIM28.

(H) GST or GST-TRIM28 RBCC alone or in the presence of untagged MAGE-A2 or untagged MAGE-C2 were bound to glutathione sepharose beads and incubated with *in vitro* translated Myc-p53. Myc-p53, MAGE-A2, and MAGE-C2 bound to the beads were detected with anti-p53, anti-MAGE-A, or anti-MAGE-C2 antibodies, respectively.

(I) MAGE-A2 and MAGE-C2 associate with UbcH2, but not UbcH5b, in cells. The indicated Myc- and HA-tagged proteins were expressed in HeLa cells and Myc-UbcH2 (1-150) or Myc-UbcH5b (1-147) were IPed with an anti-Myc antibody and HA-MAGE proteins were detected by anti-HA western blot (WB). Whole cell lysates (input) were blotted for anti-HA.

(J) GST-MAGE-A2 and GST-MAGE-C2 bind UbcH2 *in vitro*. GST-MAGE-A2 and GST-MAGE-C2 proteins were incubated with *in vitro* translated (IVT) Myc-UbcH2 (1-150) or Myc-UbcH5b (1-147). Interacting proteins were detected by anti-Myc immunoblotting.

(K) MAGE-C2 does not stimulate UbcH2 ubiquitin charging. Recombinant UbcH2 (1-150) protein was incubated for 1 hour at 30 °C in the presence or absence of His_6-Ube1 (E1), ubiquitin, Mg-ATP, and increasing concentrations of GST-MAGE-C2 as indicated. After incubation, half of the reaction was reduced in DTT containing sample buffer while the other half was solubilized in non-reducing sample buffer. Proteins were separated by SDS-PAGE and detected by coomassie staining. The ubiquitin charged UbcH2 is denoted by UbcH2~Ub.

SUPPLEMENTAL TABLE

Table S1. MAGE-RING Ligase Complexes. (Related to Figure 1)

	MAGE	RING	TAP/MS	IP/WB	*In vitro*
Type I – MAGE CTAs	MAGE-A2	TRIM28	+	+	+
	MAGE-A3	TRIM28	+		+
	MAGE-A6	TRIM28	+		+
	MAGE-B2	TRIM28	+	+	–
	MAGE-B18	LNX1	+	+	+
	MAGE-C2	TRIM28	+	+	+
Type II – Ubiquitous MAGEs	MAGE-D1	PRAJA-1		+	+
	MAGE-D1	TRIM28			+
	MAGE-D4B	TRIM27			+
	MAGE-E1	TRIM28	+	+	–
	MAGE-F1	LNX1			+
	MAGE-F1	NSE1			+
	MAGE-F1	TRIM27			+
	MAGE-G1	NSE1	+	+	+
	MAGE-G1	PRAJA-1	+		+
	MAGE-L2	TRIM27			+
	NECDIN	TRIM28	+		–

SUPPLEMENTAL EXPERIMENTAL PROCEDURES

Microarray gene expression analysis

Gene expression analysis of HCC1143, HCC1806, HTB126, and SK-BR-3 cells was performed using Affymetrix microarrays as previously described (Lam et al., 2007). For RT-QPCR analysis of gene expression, total cellular RNA was collected using the RNAeasy kit (Qiagen) according to the manufacturer's instructions. mRNA was converted to cDNA using the Superscript III reverse transcriptase (Invitrogen) in the presence of random hexamers (Invitrogen) according to manufacturer's instructions. Gene expression analysis was performed on the ABI-HT7900 (Applied Biosystems) real-time QPCR instrument. Multiplex reactions were performed using TaqMan Gene Expression Master Mix (Applied Biosystems) containing either MAGE-A3 (Hs00366532_m1) or MAGE-C2 (Hs00212255_m1) FAM-labeled TaqMan probes (Applied Biosystems) and the endogenous, normalization control VIC-GAPDH probe (Applied Biosystems; 4326317E**)**. Triplicate results from multiple experiments were analyzed using the SDS 2.2.2 software (Applied Biosystems). All samples were normalized to GAPDH expression levels.

Recombinant *in vitro* binding assays

In vitro binding assays were performed using His-TRIM28 RBCC (AA 33-413), full-length GST-MAGE-G1, untagged MAGE-B18 MHD (AA 101-331), untagged MAGE-C2 MHD (AA 140-373) and untagged full-length NSE1. 4-26 μM of the indicated proteins were incubated in binding buffer (25 mM Tris pH 8.0, 2.7 mM KCl, 137 mM NaCl, 0.05% Tween-20, 10 mM imidazole) for one hour at room temperature. Concurrently, Ni-NTA or glutathione sepharose

beads were blocked for one hour in binding buffer. Protein complexes were then captured on the blocked beads for 30 minutes at room temperature while vibrating. After 5 washes with wash buffer (25 mM Tris pH 8.0, 2.7 mM KCl, 137 mM NaCl, 0.05% Tween-20, 20 mM imidazole), the proteins were eluted with SDS-sample buffer, boiled, and subjected to SDS-PAGE and coomassie stain.

Crystallization, data collection, and structure determination

Full-length His-NSE1 and MAGE-G1 were co-expressed in BL21(DE3) *E. coli* using the pRSF-duet co-expression vector (Novagen). The protein complex was purified using a HisTrap Hp 5 ml column (GE Amersham) followed by Resource S ion exchange chromatography (GE Amersham). The His-tag was subsequently cleaved off by addition of TEV protease (Invitrogen) followed by gel filtration chromatography. The resulting MAGE-G1-NSE1 protein complex was concentrated to 15 mg/ml in 25 mM HEPES, pH 7.4, 200 mM NaCl and 5 mM DTT. The seleno-methionine derivatives of complex proteins were purified similarly.

Crystals were grown at 18 °C using the vapor diffusion method in hanging drop mode by mixing 1 µl protein with 1 µl reservoir solution (22% PEG500, Sodium Citrate pH 5.5 and 2% 1,1,1,3,3,3-Hexafluoro-2-Propanol) and equilibrating against 200 µl of reservoir solution. Crystals appeared overnight and matured in about one week. The crystals were incubated with reservoir solution supplemented with 12% (v/v) glycerol and then flash-cooled in liquid propane.

Se-SAD data were collected at the Beijing Synchrotron Radiation Facility (Beijing Electron Positron Collider, Beijing, China) at a wavelength of 0.979 Å using a MAR165 (MAR Research, Hamburg) CCD detector at 100 K and processed with HKL2000 (Otwinowski and Minor, 1997). Native data were collected at the Spring-8 beamline BL38B1, which were integrated and scaled with the program XDS (Kabsch, 1988). Further processing was carried out

using programs from the CCP4 suite (Collaborative Computational Project, 1994). Data collection statistics are summarized in Table 1.

The selenium sites were located using SHELXD (Schneider and Sheldrick, 2002) from the Bijvoet differences in the Se-SAD data. Heavy atom positions were refined and phases calculated with PHASER's SAD experimental phasing module (McCoy et al., 2007). The real-space constraints were applied to the electron density map in DM (Cowtan, 1994). Several secondary structural features could be recognized in the resulting map. However, model building was only possible when using cross-crystal averaging to improve the phases, because the high-resolution native data set was non-isomorphous with the Seleno-Methionine data set. Three rough masks were calculated around the NSE1 molecule and two MAGE-G1 subunits: MAGE-G1-1 (residues 78-159) and MAGE-G1-2 (residues 173-293). Cross-crystal averaging combined with solvent flattening and histogram matching was then performed in DMMulti (Cowtan, 1994). Although the resulting map was of sufficient quality for model building of the NSE1 and MAGE-G1-1 molecules, the density around MAGE-G1-2 was not good enough to build the accurate model. Fortunately, Zinc atoms in the native data set also showed significant anomalous signal at the wavelength of 1.0 Å, which was treated as another SAD data independently. The Zn-SAD phases were then combined with the phases transferred from the Se-SAD data, which gave maps of sufficient quality to build the initial model for the whole molecule in COOT (Emsley and Cowtan, 2004). The structure was refined with the PHENIX (Adams et al., 2002) packages.

Tandem affinity purification and mass spectrometry

For large scale purification, ten 150 mm^2 dishes of 293/TAP-MAGE stable cells were harvested in TAP-lysis buffer (10% glycerol, 50 mM HEPES-KOH pH 7.5, 100 mM KCl, 2 mM ethylenediaminetetraacetic acid (EDTA), 0.1% NP-40, 10 mM NaF, 0.25 mM NA_3VO_4, 50 mM β-glyerolphosphate, 2 mM dithiothreitol (DTT), and 1X protease inhibitor cocktail). Cleared lysates were bound to IgG-Sepharose beads (GE Amersham) for 4 hrs at 4°C. Beads were subsequently washed three times in lysis buffer and TEV buffer (10 mM HEPES-KOH pH 8.0, 150 mM NaCl, 0.1% NP-40, 0.5 mM EDTA, 1 mM DTT, and 1X protease inhibitor cocktail). Protein complexes were cleaved off the beads by 70 µg TEV protease in TEV buffer overnight at 4 °C. Supernatants were diluted in calmodulin binding buffer (10 mM HEPES-KOH pH 8.0, 150 mM NaCl, 1 mM Mg acetate, 1 mM imidazole, 0.1% NP-40, 6 mM $CaCl_2$, 10 mM 2-mercaptoethanol) and incubated with calmodulin-sepharose beads (GE Amersham) for 90 minutes at 4 °C. Captured protein complexes were washed three times in calmodulin binding buffer and calmodulin rinse buffer (50 mM ammonium bicarbonate pH 8.0, 75 mM NaCl, 1 mM Mg acetate, 1 mM imidazole, 2 mM $CaCl_2$). Proteins were eluted in 2X sodium dodecyl sulfate (SDS) sample buffer, boiled for 10 min, concentrated in microcon concentrators (Millipore), and subjected to SDS-polyacrylamide gel electrophoresis (PAGE). Gels were stained with colloidal coomassie blue stain (Peirce) according to manufacturer's protocol.

Unique bands were excised and in-gel proteolysis was performed using modified porcine trypsin digestion overnight. The resulting peptide mixture was dissolved and subjected to nano-LC/MS/MS analysis on a ThermoFinnigan LTQ instrument, coupled with an Agilent 1100 Series HPLC system. Peptide sequences were identified using the Mascot search engine (Matrix science). Those proteins identified in the TAP-MAGE purification with multiple peptides and not identified in the TAP-vector only control pull-downs were considered hits.

SUPPLEMENTAL REFERENCES

Adams, P.D., Grosse-Kunstleve, R.W., Hung, L.W., Ioerger, T.R., McCoy, A.J., Moriarty, N.W., Read, R.J., Sacchettini, J.C., Sauter, N.K., and Terwilliger, T.C. (2002). PHENIX: building new software for automated crystallographic structure determination. Acta. Crystallogr. D. Biol. Crystallogr. *58*, 1948-1954.

Carson, J.P., Zhang, N., Frampton, G.M., Gerry, N.P., Lenburg, M.E., and Christman, M.F. (2004). Pharmacogenomic identification of targets for adjuvant therapy with the topoisomerase poison camptothecin. Cancer Res. *64*, 2096-2104.

Collaborative Computational Project, N. (1994). The CCP4 suite: programs for protein crystallography. Acta. Crystallogr. D. Biol. Crystallogr. *50*, 760-763.

Cowtan, K. (1994). dm: An automated procedure for phase improvement by density modification. Jnt. CCP4/ESF-EACBM Newsl. Protein Crystallogr. *31*, 34-38.

El Hader, C., Tremblay, S., Solban, N., Gingras, D., Beliveau, R., Orlov, S.N., Hamet, P., and Tremblay, J. (2005). HCaRG increases renal cell migration by a TGF-alpha autocrine loop mechanism. Am. J. Physiol. Renal. Physiol. *289*, F1273-1280.

Elkon, R., Rashi-Elkeles, S., Lerenthal, Y., Linhart, C., Tenne, T., Amariglio, N., Rechavi, G., Shamir, R., and Shiloh, Y. (2005). Dissection of a DNA-damage-induced transcriptional network using a combination of microarrays, RNA interference and computational promoter analysis. Genome Biol. *6*, R43.

Emsley, P., and Cowtan, K. (2004). Coot: model-building tools for molecular graphics. Acta. Crystallogr. D. Biol. Crystallogr. *60*, 2126-2132.

Kabsch, W. (1988). Evaluation of single-crystal X-ray diffraction data from a position-sensitive detector. J. Appl. Crystallogr. *21*, 916-924.

Kim, H.S., Kim, M.S., Hancock, A.L., Harper, J.C., Park, J.Y., Poy, G., Perantoni, A.O., Cam, M., Malik, K., and Lee, S.B. (2007a). Identification of novel Wilms' tumor suppressor gene target genes implicated in kidney development. J. Biol. Chem. *282*, 16278-16287.

Kim, Y.K., Furic, L., Parisien, M., Major, F., DesGroseillers, L., and Maquat, L.E. (2007b). Staufen1 regulates diverse classes of mammalian transcripts. EMBO J. *26*, 2670-2681.

Lam, D.C., Girard, L., Ramirez, R., Chau, W.S., Suen, W.S., Sheridan, S., Tin, V.P., Chung, L.P., Wong, M.P., Shay, J.W., *et al.* (2007). Expression of nicotinic acetylcholine receptor subunit genes in non-small-cell lung cancer reveals differences between smokers and nonsmokers. Cancer Res. *67*, 4638-4647.

McCoy, A.J., Grosse-Kunstleve, R.W., Adams, P.D., Winn, M.D., Storoni, L.C., and Read, R.J. (2007). Phaser crystallographic software. J. Apple. Crystallogr. *40*, 658-674.

Monroe, D.G., Secreto, F.J., Subramaniam, M., Getz, B.J., Khosla, S., and Spelsberg, T.C. (2005). Estrogen receptor alpha and beta heterodimers exert unique effects on estrogen- and tamoxifen-dependent gene expression in human U2OS osteosarcoma cells. Mol. Endocrinol. *19*, 1555-1568.

Otwinowski, Z., and Minor, W. (1997). Processing of X-ray diffraction data collected in oscillation mode. Methods Enzymol. *276*, 307-326.

Schneider, T.R., and Sheldrick, G.M. (2002). Substructure solution with SHELXD. Acta. Crystallogr. D. Biol. Crystallogr. *58*, 1772-1779.